International Workshop on Deep Structure,
Singularities and Computer Vision
(DSSCV 2005): 60-71

Estimating the Statistics of Multi-Object Anatomic Geometry Using Inter-Object Relationships

Stephen M. Pizer, Ja-Yeon Jeong, Conglin Lu, Keith Muller, and Sarang Joshi

Medical Image Display & Analysis Group (MIDAG)
University of North Carolina, Chapel Hill NC 27599, USA

Abstract. We present a methodology for estimating the probability of multi-object anatomic complexes that reflects both the individual objects' variability and the variability of the inter-relationships between objects. The method is based on m-reps and the idea of augmenting medial atoms from one object's m-rep to the set of atoms of an object being described. We describe the training of these probabilities, and we present an example of calculating the statistics of the bladder, prostate, rectum complex in the male pelvis. Via examples from the real world and from Monte-Carlo simulation, we show that this means of representing multi-object statistics yields samples that are nearly geometrically proper and means and principal modes of variations that are intuitively reasonable.

1 Introduction

Since multiple objects form a given anatomic region, there has been a desire to characterize probabilistically populations of multi-object anatomic geometry. Our companion paper [2] makes the case that probabilities on populations of geometric regions are an essential part of multiscale probabilities on geometric-model-based image intensities. In the schema described there regions of space with predictable intensity histograms are placed in a neighbor relationship, and this is done at a number of different discrete scale levels. In another of our papers [5], three scale levels are under consideration: that global to the image, that consisting of only objects without interstitial regions, and that consisting of certain through-object subsections. Here we assume the ability to handle the global scale level and through-object subsection scale level, and we focus on the critical issue of how to produce probability distributions that reflect not only region (object) shape but also inter-object geometric relationships.

The approaches to forming probability distributions on multi-object anatomic geometry that have been tried so far consist of representing the objects and doing global statistics on these representations, as derived from some dozens of training cases. Among the representations to which this approach has been applied are point distribution models [3], diffeomorphisms from atlases [14], distance functions or their levels sets [7], and our own m-reps [1]. We suggest that such global statistics pay inadequate attention to the objects themselves and most

especially to the inter-relations among objects. We provide a concrete method that generates probabilities directly on objects and their relationships.

M-reps are representations of object interiors that consist of hierarchies of sheets of medial atoms. They are designed to have the following properties: 1) By medial atom transformations they explicitly capture local bending and twisting (rotation), local magnification, and local elongation, and they separate these from one another. 2) They are based on the subdivision of an object into figures, i.e., main bodies, protrusions, and indentations. Moreover, they provide a fixed topology of such branching for a population of objects and thus allow statistics on this population. 3) They provide a local coordinate system for object interiors that can provide correspondences across instances of an object. 4) They allow neighboring geometric entities to be understood as medial atom transformations of each other. This allows rich characterization of neighbor relationships, for situations internal to a figure, between figures, or between objects.

We use m-reps as the geometric models and statistics using geodesic distance on the curved manifold of a symmetric space [4]. Here we restrict the discussion to objects each of which can be represented by a single sampled sheet of medial atoms (Fig. 1), i.e., "single-figure objects". We show examples describing the variability of the bladder, prostate, and rectum complex in the male pelvis within a patient across a series of treatment days.

We assume that we are given a single-figure m-rep model for multiple objects, for many training cases, and we assume further that the object complexes have already been aligned across the cases and that the medial atoms correspond across the cases.

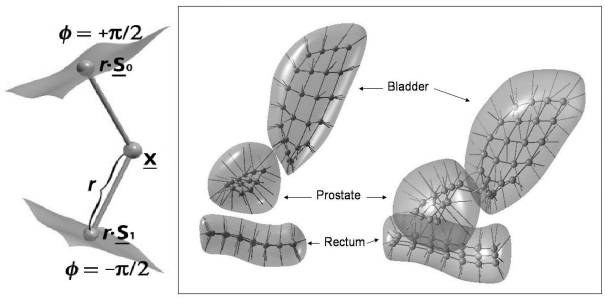

Fig. 1. Medial atom with a section of implied boundary surface (left). An m-rep 3-object complex for the bladder, the prostate, and the rectum of a patient in different view in a box (right).

Limiting ourselves here to the object level of locality, we assume that any truly global variation of the complex has been removed from each object, via the residue technique described in [5]. We do not consider the interstitium between and around objects.

The subject of sections 2-6 is how to express and compute the probabilities of the objects and of the inter-object geometry. In section 2 we overview the approach and then in succession treat its three major components, namely section 3: atom augmentation to simultaneously capture objects and their relations to other objects, section 4: propagation of the inter-object relations to remaining objects, and section 5: inter-object residues to describe the variation remaining after the propagation of effects from other objects. In section 6 we explain how to train probabilities for objects by successive PGA's on object residues.

We say that a geometric model for a complex of non-interpenetrating objects is *proper* if a) the topology of the objects is retained, b) each object in the model does not have singularities or folds of its boundary or interior, and c) the non-interpenetration of objects is retained within the tolerances appropriate for the scale of the description. Many previous methods for estimating inter-object probability distributions have produced samples some of which are decidedly improper. In section 7 we test our method by illustrating that models sampled from our probability distributions on intra-patient bladder, prostate, and rectum deformations are nearly proper and that the means and principal modes of variation of these distributions are intuitively reasonable. We also briefly discuss application of these ideas to segmentation by posterior optimization. Section 8 discusses further opportunities for evaluation, and extensions and alternatives to the proposed methods.

2 Overview of the approach

We assume that in each case we have n objects, with m-reps $\underline{\mathbf{z}}^2 = \{M_k\}_{k=1}^n$ where M_k is an ordered set of medial atoms and $\underline{\mathbf{z}}^2$ describes the geometric representation of objects at the second scale level as in [2]. Each interior medial atom requires an 8-tuple to represent, describing a hub and two equal-length spokes (Fig. 1), and each grid-edge medial atom requires a 9-tuple to represent, describing a hub, two equal-length spokes, and a third spoke formed from their bisector, which may be of a different length. In our present approach we assume that the objects will be provided in an order of decreasing stability, i.e., whose posterior probability, based on both geometric and intensity variability and edge sharpness, are in decreasing levels of tightness. In this work we provide object statistics in this order, treating each object once. The details of dealing with these objects' statistics in sequence are described in section 6. In section 8 we discuss the extension to a form of a Markov process described in [2].

The main new idea of this paper (Fig. 2) is that while estimating the statistics of a particular object M_k we deal with that object's inter-relation with other atoms by augmenting highly correlated atoms A_k in the remaining objects $R_k = \cup_{i>k}(M_i)$ to M_k to produce "augmented" representations $U_k = M_k \cup A_k$. We can write $p(\underline{\mathbf{z}}^2) = p(U_k, R_k) = p(U_k)p(R_k|U_k)$. In specifying $p(R_k|U_k)$, we divide the effect into a deterministic prediction from U_k and an U_k-independent probability on the residue of R_k from that prediction. When comparing this to the equation in the companion paper [2], $p(\underline{\mathbf{z}}_k^2 \mid \underline{\mathbf{z}}_{N(2,k)}) =$

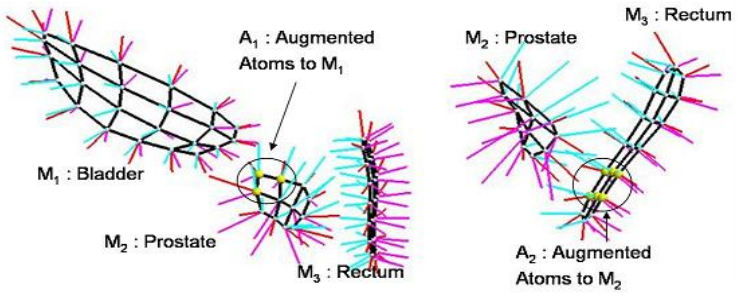

Fig. 2. A discrete m-rep for the bladder (M_1), the prostate (M_2), the rectum (M_3) 3-object complex of a patient. The augmented atoms in the prostate forming A_1 are shown with their hub enlarged (left). The prostate (M_2), the rectum (M_3) of the same patient the enlarged atoms in the rectum form A_2 (right).

$p(\text{shape of } \underline{\mathbf{z}}_k^2, \text{ inter-relation of } \underline{\mathbf{z}}_k^2, \text{ and } \underline{\mathbf{z}}_{N(2,k)})$, we see that in effect we are describing the shape of R_k by its residue and the interrelation with M_k via U_k.

We now describe the other aspect of our new idea, the deterministic propagation of augmenting atoms' movement in the statistics of one augmented object to the remainder of the objects to be processed. The idea is that if an object changes position, pose, size, or shape, its neighboring objects will change sympathetically. In particular (Fig. 3), let all of the atoms in these other objects whose statistics are yet to be determined be R_k. The changes in A_k will be reflected in sympathetic changes in $R_k \setminus A_k$ [1] before the statistics on $R_k \setminus A_k$ are calculated. The details of this propagation are discussed in section 4.

We synthesize these probability distributions via principal geodesic analysis (PGA)[4]. This method of augmentation is discussed further in section 3.

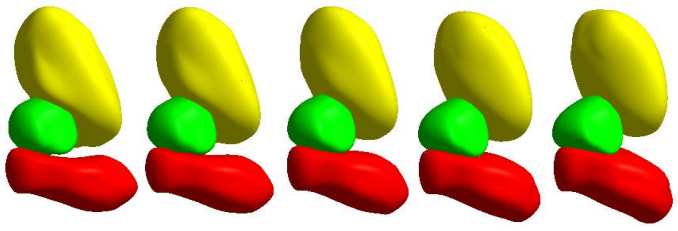

Fig. 3. Assuming we have produced statistics for the augmented bladder U_1, which has augmenting atoms A_1 in the prostate (M_2), we illustrate the sympathetic change of $R_1 \setminus A_1$ caused by A_1.

[1] Recall that the notation $A \setminus B$ means the set difference A minus B.

3 Objects inter-relation by augmentation

Because we have evidence that atoms in one object that are near another object are most highly correlated with that other object, we describe the inter-relation of a multi-object using these nearby atoms for augmentation. In the male-pelvis example of Fig. 2, medial atoms in bladder M_1 should be more highly correlated with medial atoms nearby in prostate A_1 than those in the rest of the prostate or in the rectum $R_1 \setminus A_1$. Thus we let the nearby prostate atoms form A_1, producing the representation of the augmented bladder U_1. We study the effect of the deformation of the bladder on the augmenting atoms and then study the relation of changes in the augmenting atoms A_1 to that of rest of the prostate and the rectum, $R_1 \setminus A_1$. We use the latter results in a stage we call prediction, which is explained next.

4 Prediction of movements from augmentation by using the shape space of the remaining objects

In prediction we reflect a change in M_k in the statistics of R_k by predicting how $R_k \setminus A_k$ bends, twists or warps from the change of M_k through augmenting atoms A_k. In doing so, we take account of the shape space of the remainder objects R_k as suggested in [6], but using PGA in a nonlinear symmetric space rather than the principal component analysis used in [6].

Recall that PGA involves first finding the mean μ of m-reps $\{\mathbf{M}_i \in \mathcal{M}\}_{i=1}^N$, where $\mathcal{M}$ is the symmetric space of an m-rep $\mathbf{M}_i$ and N is the number of training cases; projecting $\{\mathbf{M}_i\}_{i=1}^N$ to the tangent space $T_\mu\mathcal{M}$ at μ by the log map[2] ($\log_\mu : \mathcal{M} \to T_\mu\mathcal{M}$); and then doing PCA in the tangent space, which yields a set of principal directions $\{v_l\}_{l=1}^h$ in $T_\mu\mathcal{M}$. Taking the exponential map ($\exp_\mu : T_\mu\mathcal{M} \to \mathcal{M}$) of $\{v_l\}_{l=1}^h$ gives a set of principal geodesics in $\mathcal{M}$, which in turn generates a submanifold $\mathcal{H}$ of $\mathcal{M}$. $\mathcal{H}$ is the shape space in which different modes of variations restricted to $\mathcal{H}$ of $\{\mathbf{M}_i\}_{i=1}^N$ are described via principal geodesics. The projection of $\mathbf{M}_i$ onto the shape space $\mathcal{H}$, $Proj_{\mathcal{H}}(\mathbf{M}_i)$[3], describes the unique variation within $\mathcal{H}$ nearest in geodesic distance to $\mathbf{M}_i$.

Now consider the augmented m-rep object $U_k = (M_k \cup A_k)$ and R_k ($A_k \subset R_k$). Let μ_r and H_r be the mean and the shape space generated by principal geodesics in the symmetric space $\mathcal{M}_r$ of R_k, which we can obtain by performing PGA on training cases of R_k. If we know how U_k deforms, i.e., how M_k and A_k change together, $Proj_{\mathcal{H}_r}(A_k)$ predicts how the remaining object R_k changes sympathetically through A_k in the shape space H_r:

$$Proj_{\mathcal{H}_r}(A_k) = \exp_{\mu_r}\left(\sum_{l=1}^{h_r}\langle \log_{\mu_r}(A_k), v_l\rangle \cdot v_l\right), \tag{1}$$

[2] Refer to [4] for detailed explanation of the log map and the exponential map.

[3] More precisely, the projection operator $Proj_{\mathcal{H}} : \mathcal{M} \to \mathcal{H}$ is approximated by $Proj_{\mathcal{H}}(\mathcal{M}) = \exp_\mu\left(\sum_{l=1}^{h}\langle \log_\mu(\mathcal{M}), v_l\rangle \cdot v_l\right)$. For detailed explanation, refer to [4].

where $\{v_l\}_{l=1}^{h_r}$ are principal directions in the tangent space at μ_r corresponding to the principal geodesics in H_r and the dimension of $\log_{\mu_r}(A_k)$ is adjusted to match with that of v_l by adding zeros to $\log_{\mu_r}(A_k)$ for parameters corresponding to $R_k \setminus A_k$. Then the prediction for the remainder R_k can be defined as

$$Pred(R_k;\, A_k) := Proj_{\mathcal{H}_r}(A_k)\ . \tag{2}$$

Notice that $Pred(R_k;\, A_k)$ is also an m-rep.

5 Residues of objects in order

If we describe the changes in U_k and the sympathetic changes in $R_k \setminus A_k$, all that is left to describe statistically is the remaining changes in R_k after the sympathetic changes have been removed. If the objects are treated in order and each object has augmenting atoms only in the next object, this will mean that n probability distributions will need to be trained, namely, for U_1, for U_2 after the sympathetic changes from U_1 have been removed, ... , for U_n after the sympathetic changes from $U_1, U_2 \ldots$, and U_{n-1} have been removed. The removal of sympathetic changes is accomplished via the residue idea described in [5]. Next we explain how such residues are calculated between a predicted remainder $\mathbf{N}^0$ and the actual value $\mathbf{M}$ of that remainder.

5.1 Difference of medial atoms

A medial atom $\mathbf{m} = (\mathbf{x},\, r,\, \mathbf{u}, \mathbf{v})$ is defined as an element of the symmetric space $G = R^3 \times R^+ \times S^2 \times S^2$ where the position $\mathbf{x} \in R^3$, the spoke length $r \in R^+$, and two unit spoke directions $\mathbf{u}, \mathbf{v} \in S^2$ (S^2 is a unit sphere). If an m-rep has d medial atoms, the m-rep parameter space becomes $\mathcal{M} = G^d$. Let $\mathbf{R_w}$ represent the rotation along the geodesics in S^2 that moves a point $\mathbf{w} \in S^2$ to the north pole $\mathbf{p} = (0, 0, 1) \in S^2$. For given any two medial atoms $\mathbf{m}_1, \mathbf{m}_2 \in G$ where $\mathbf{m}_i = (\mathbf{x}_i,\, r_i,\, \mathbf{u}_i, \mathbf{v}_i)$, $i = 1, 2$, the difference between them can be described as follows:

$$\begin{gathered} \ominus : G \times G \longrightarrow G \\ \mathbf{m}_1 \ominus \mathbf{m}_2 := (\mathbf{x}_1 - \mathbf{x}_2,\, \tfrac{r_1}{r_2},\, \mathbf{R}_{\mathbf{u}_2}(\mathbf{u}_1)\, \mathbf{R}_{\mathbf{v}_2}(\mathbf{v}_1))\ . \end{gathered} \tag{3}$$

$\mathbf{m}_1 \ominus \mathbf{m}_2$ is the difference between $\mathbf{m}_1, \mathbf{m}_2$ relative to $\mathbf{m}_2$ coordinates. Like $\mathbf{m}_1$ and $\mathbf{m}_2$, $\mathbf{m}_1 \ominus \mathbf{m}_2 \in G$.

Corresponding to the difference operator $\ominus$, the addition operator $\oplus$ can be defined as:

$$\begin{gathered} \oplus : G \times G \longrightarrow G \\ \mathbf{m} \oplus \Delta\mathbf{m} := (\mathbf{x} + \Delta\mathbf{x},\, r \cdot \Delta r,\, \mathbf{R}_{\mathbf{u}}^{-1}(\Delta\mathbf{u}),\, \mathbf{R}_{\mathbf{v}}^{-1}(\Delta\mathbf{v})) \end{gathered} \tag{4}$$

for given $\mathbf{m} = (\mathbf{x},\, r,\, \mathbf{u}, \mathbf{v})$ and the difference $\Delta\mathbf{m} = (\Delta\mathbf{x},\, \Delta r,\, \Delta\mathbf{u}, \Delta\mathbf{v})$. This operation is neither commutative nor associative. As an m-rep object is a collection of medial atoms, these operations can be individually applied to each atom of the object.

5.2 Residues in an object stage

Our probabilistic analysis proceeds object by object in order. After some object has been described probabilistically and its sympathetic effect has been applied to its remainder, there is a further change in the remaining objects to be described. We call that further change the residue of the remainder objects with respect to the probability distribution on the first. More precisely, let $\mathbf{M} \in \mathcal{M}$ be an m-rep or an m-rep residue of one object fitting a particular training case where $\mathcal{M}$ is a symmetric space of $\mathbf{M}$ and let $p(\mathbf{N})$ be a probability distribution on $\mathbf{N} \in \mathcal{M}$ describing part of the variation of $\mathbf{M}$. Notice that if $D(p)$ represents the domain of p, then $D(p)$ is a submanifold of $\mathcal{M}$. Relative to the probability distribution p, $\mathbf{N}^0$, the closest m-rep to $\mathbf{M}$ in $D(p)$, is

$$\mathbf{N}^0 = \arg \min_{\mathbf{N} \in D(p)} d(\mathbf{M}, \mathbf{N}), \tag{5}$$

where $d(\mathbf{M}, \mathbf{N})$ is the geodesic distance on $\mathcal{M}$. Then the residue $\Delta\mathbf{M}$ of $\mathbf{M}$ with respect to p can be defined as

$$\Delta\mathbf{M} := \mathbf{M} \ominus \mathbf{N}^0 \ . \tag{6}$$

In the method we are describing, we use the prediction $Pred(\mathbf{M}; \mathbf{A})$ from a set of augmented atoms $\mathbf{A}$ in $\mathbf{M}$ to $\mathbf{M}$'s previous object (of which movements have an effect on $\mathbf{M}$) as an approximation to $\mathbf{N}^0$ because the prediction is made on the shape space of $\mathbf{M}$ and the augmentation can give a good estimation to the overall effect of $\mathbf{M}$'s previous object. We expect the prediction $Pred(\mathbf{M}; \mathbf{A})$ to be close to $\mathbf{N}^0$. Thus we compute $\Delta\mathbf{M} := \mathbf{M} \ominus Pred(\mathbf{M}; \mathbf{A})$.

6 Training the probabilities for objects

Training the probabilities for the object is done via successive PGA's on the object residues. Using the notation from Sec. 2, let O^i be a multi-object m-rep residue in case i from which any truly global variations are removed from $\{M_k^i\}_{k \in K}$, where $I = \{1, \ldots, N\}, K = \{1, \ldots, n\}$ are index sets for N training cases and n objects. Then $O^i = \{\Delta M_k^i\}_{k \in K}$ forms a multi-object m-rep residue of the i^{th} training case.

The residues $\{O^i\}_{i \in I}$ are treated in the order of objects M_k from $k = 1$ to n. First we apply PGA on $\{\Delta U_1^i\}_{i \in I}$, the residue of the first object, to get the mean μ_1 and a set of principal variances and associated principal geodesics $\{\exp_{\mu_1}(v_1^l)\}_{l=1}^{n_1}$, where $v_1^l \in T_{\mu_1}\mathcal{M}_1$. This mean, principal variances, and principal geodesics provide our estimate of the probability distribution of ΔU_1. Let $\mathcal{H}_1$ be a submanifold of $\mathcal{M}_1$, where $\mathcal{M}_1$ is the symmetric space for ΔU_1. The projection of ΔU_1^i onto the geodesic submanifold $\mathcal{H}_1$, $Proj_{\mathcal{H}_1}(\Delta U_1^i)$, describes the variation unique to ΔU_1^i in $\mathcal{H}_1$. Now we need to update the residue $\{\Delta R_1^i\}_{i \in I}$ to reflect the sympathetic effect from ΔM_1 on ΔR_1 by ΔA_1. That is done using the prediction $Pred(\Delta R_1^i;\ \Delta A_1^i)$ as described in Sec. 4.

So the residue for the next object (the second object) that we use to apply PGA is no longer $\{O^i\}_{i\in I}$. The updated residue of the remainder to the first object becomes

$$\Delta^2 R_1^i = \Delta R_1^i \ominus Pred(\Delta R_1^i;\ \Delta A_1^i) \qquad i \in I\ . \tag{7}$$

Once we have the new updated residue $\Delta^{k-1}U_k^i \subset \Delta^{k-1}R_k^i$ for the k^{th} object, $k = 2, \ldots, n$, we repeat the same steps 1) applying PGA on $\Delta^{k-1}U_k^i$ and 2) updating the residue of the remainder, which produces a set of means $\{\mu_k\}_{k\in K}$ and sets of principal geodesics $\{\{\exp_{\mu_k}(v_k^l)\}_{l=1}^{n_k}\}_{k\in K}$ on object residues.

7 Geometrically proper objects in probability distributions in the male pelvis

Samples being geometrically improper has been a problem for other methods such as PCA on distance functions or on dense PDMs. Examples of what we mean by geometrically improper is wrong topology, interpenetration of separated objects, folding, and singularities such as unwanted corners and cusps. There are two reasons why we would expect that our methods would avoid geometrically improper samples from their probability distributions.

1) M-reps are founded on the idea that using primitive transformations including local twisting and bending of objects will yield an economical representation of the single and multi-object transformations of anatomy between individuals or within an individual over time. When using such transformations in the representation methods and in particular in the methods of description of object inter-relations via augmentation and prediction, nonlinear PGA is necessary to produce sample object complexes that are geometrically proper.

2) The regular grids of medial atoms that we generate from training binary images of objects [9] are designed to have large geodesic distance to improper entities on the manifold $\mathcal{M}$. Thus we might hope that objects within $[-2, +2]$ standard deviations will also be proper. Analysis of our objects using a criterion based on the radial shape operator of [8] could be used to avoid improper models, but this criterion has not been applied in the work described in this paper.

The most basic test of our probability distributions is to visually judge whether those generated samples are proper and whether the principal geodesic directions derived from real patient data explain variations we see in the training samples. Because our training set is just a particular sample subset of a population of m-reps, we wish to know how our method would fare on other training sample subsets. We can accomplish this by generating new random samples from our probability distributions and test whether training from these samples produces a probability distribution whose samples are proper.

We generate the new samples by assuming that each tangent plane principal component from the original training follows the standard normal distribution once we scale the principal directions by the square root of corresponding eigenvalues in the tangent space. Thus, for each object residue we randomly sample

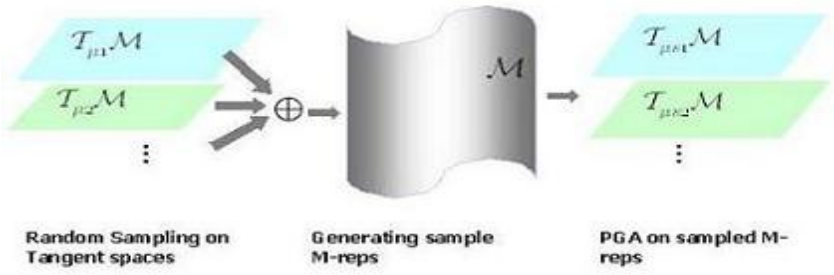

Fig. 4. Left: tangent spaces at object residue means from real patient data. Middle: m-rep parameter space. Right: object residue means from generated training data. The movie of 100 sampled m-reps from patient 1 and patient 2 data is at `http://www.cs.unc.edu/~jeong/DSSCV05/100SamplesPat1and2.avi`. In the movie the point of view changes from time to time.

each principal component following the standard normal distribution to generate random points on each tangent space about the mean $\{\mu^k\}_{k\in J}$. By taking exponential maps of those points, we generate m-reps and residues that can be combined by $\oplus$ to produce new training sample m-reps. PGA on such a new sampled training set yields a new mean and set of principal directions and variances, whose samples we can judge as to how proper they are.

We applied our new method to obtain the probability distributions from two training sets, each of which are obtained from bone-aligned male-pelvis CT images of a real patient over several days. A single-figure m-rep was fit to each organ: 4x6 grids of medial atoms for the bladder, 3x4 grids for the prostate, and 3x7 grids for the rectum. The total number of medial atoms is 57, so the dimension of the m-rep parameter space is 456. Our software to fit the single figure m-reps to binary image of each organ provides reasonable correspondence of medial atoms across cases by penalizing irregularity and rewarding correspondence to one case [9]. Inter-penetrations among m-reps of the three objects were restricted in the fitting [9] of each training case. We have 11 cases (m-reps) of one patient (patient 1) and 17 cases of another patient (patient 2).

Figure. 5 displays the first modes of variation of patient 1 and 2 at PGA coefficients -2, -1, 1, 2 standard deviations of bladder with prediction, prostate with prediction and rectum in Fig. 5 from the top row to the bottom row.

In these movies, as well as the ones seen in fig. 4, we see the following behaviors: 1) The m-reps produced as samples or chosen along principal geodesics yield limited inter-object penetration, as desired since the training samples have small inter-object penetration. 2) The surfaces of the m-rep sample implied objects are smooth, with few exceptions. Folding is not observed, and the introduction of sharp ridges happens seldom, only at crest positions which are sharp in some of the training cases. 3) The principal geodesics seem to correspond to anatomically

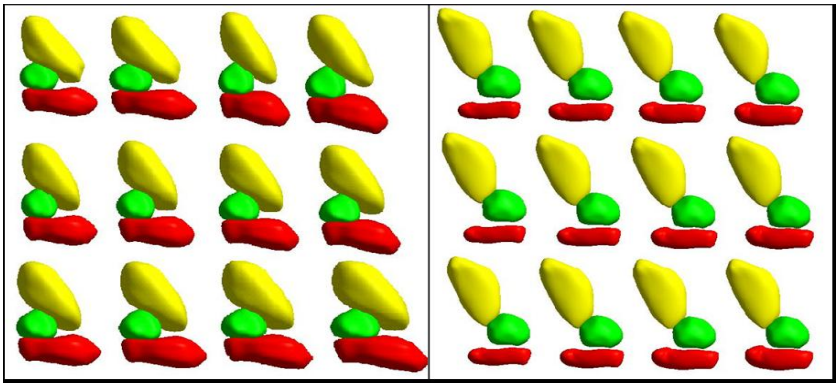

Fig. 5. Illustration of first modes of variation of patient 1 in the box on the left and that of patient 2 in the box on the right. The movie that shows the first modes of variations of patient 1 and then patient 2 is at `http://www.cs.unc.edu/~jeong/DSSCV05/VariationsPat1and2.avi`.

observed changes. For example, we see strong growth in the bladder corresponding to filling and strong bulging of the rectum corresponding to the introduction of bowel gas. Also, the prostate residue shows only modest shape changes, a behavior expected from the fact that the prostate is typically quite hard.

It is in this sense that we say that our statistical method provides samples that are "nearly geometrically proper and means and principal modes of variations that are intuitively reasonable."

In addition to the evaluation of m-rep probabilities just described, we can also judge the probabilities by their usefulness in segmentation. In particular, these probabilities are used as the prior at the object scale level in segmentation by 3-scale (global, object, medial atom) posterior optimization of m-reps of the bladder, prostate, rectum complex. These probabilities are trained from images of a given patient on a variety of days, and the segmentation method is applied to new target images of the same patient on different days. The details of the application to segmentation are given in [2] and [12], object segmentation using histogram statistics is described in [15], and the results on a few cases, agreeing well with human segmentations, have been reported in [13]. Briefly, the results are anecdotal but encouraging.

8 Discussion and Conclusion

We presented new ideas in estimating the probability distribution of multi-object anatomic objects via augmentation and prediction with principal geodesic analysis suggested in [4]. As described in our companion paper [2], a schema involving neighboring regions at multiple scales has much to recommend it. At each scale

level in this schema, except the global level, a means is needed to produce statistics reflecting region shape and inter-region relations for neighboring regions. This paper has shown the viability of a particular method for producing these statistics.

We have also applied our approach of augmentation and prediction to compute statistics of m-reps of multi-figure objects, the structure of which is described in [10]. We take hinge atoms as augmented atoms and predict the sympathetic change of a subfigure from the change of its host figure [11].

In this paper, we have limited the residue to the object level of locality. But we can compute finer residues at the medial atom level of locality and do further analysis as described in [5].

Other evaluations of the sample probability distributions generated using Monte Carlo approaches to generate new sample training sets are in progress. These involve measuring the bias and reliability of the resulting probability distributions and determining the number of training samples required.

We can avoid ordering the objects by considering the mutual neighbor relation in augmentation. This extension from the present approach to the Markov Random Field approach as discussed in [2] is suggested by real situations such as male-pelvis example that we used: not only can the bladder induce a change in the prostate and rectum but also the change of a prostate can induce sympathetic change in the bladder and rectum, etc.

We have chosen the augmented atoms based on the distance between atoms in one object and the other because we have preliminary evidence done by [5] that those nearby atoms are highly correlated. Another test needed is whether the remaining atoms are independent of the primary object when conditioned on the augmenting atoms. In addition, attention is needed to defining the global statistics so that the object probabilities and the global probabilities are conditionally independent of each other. In this way the global probabilities will not simply involve principal geodesic analysis of $\cup_{k=1}^{n} M_k$.

The success of geodesic statistics depends on the initial alignment of the training cases. In the example used in this paper, a global alignment of the cases was accomplished using a rigid object, the pelvic bones. In multi-patient cases, however, the alignment needs to be accomplished by the Procrustes algorithm using the geodesic distance metric [4]. Once the global statistics have been computed, it may be desirable to realign for each object, before the residue for that object is analyzed.

Finally, a possible measure to explain the inter-object relation is canonical correlation. Canonical correlation explains the relation of two sets of variables each in a linear space. Here we wish to relate M_k and its neighbors. Because the principal geodesics are defined in tangent spaces to the symmetric space $\mathcal{M}$, we speculate that we can incorporate this canonical correlation directly as an alternative to the method described in this paper.

We thank Edward Chaney, Gregg Tracton, and Derek Merck for pelvis models. This work was done under the partial support of NIH grant P01 EB02779.

References

1. S.M. Pizer, T. Fletcher, Y. Fridman, D.S. Fritsch, A.G. Gash, J.M. Glotzer, S. Joshi, A. Thall, G Tracton, P. Yushkevich, and E.L. Chaney, "Deformable M-Reps for 3D Medical Image Segmentation," *International Journal of Computer Vision* - Special UNC-MIDAG issue, (O Faugeras, K Ikeuchi, and J Ponce, eds.), vol. 55, no. 2, pp. 85-106, Kluwer Academic, November-December 2003
2. S.M. Pizer, JY. Jeong, R. Broadhurst, S. Ho, and J. Stough, "Deep Structure of Images in Populations via Geometric Models in Population," in *this volume, International Workshop on Deep Structure, Singularities and Computer Vision (DSSCV)*, 2005.
3. T.F. Cootes, C.J. Taylor, D.H. Cooper, and J. Graham, "Active Shape Models Their Training and Application," *Computer Vision and Image Understanding*, Elsevier, Vol. 61 (1995), No. 1, pp.38-59.
4. P.T. Fletcher, C. Lu, S.M. Pizer, and S. Joshi, "Principal Geodesic Analysis for the Study of Nonlinear Statistics of Shape," *IEEE Transactions on Medical Imaging*, vol. 23, no. 8, pp. 995-1005, IEEE, Aug. 2004.
5. C. Lu, S.M. Pizer, and S. Joshi, "Statistical Multi-object Shape Models," *in preparation.*
6. K. Rajamani, S. Joshi, and M. Styner, "Bone model morphing for enhanced surgical visualization," in *International Symposium on Biomedical Imaging*, pp.1255-1258, Apr. 2004.
7. A. Tsai, A. Yezzi, W. Wells, C. Tempany, D. Tucker, A. Fan, E. Grimson, and A. Willsky, "A Shape-Based Approach to Curve Evolution for Segmentation of Medical Imagery," *IEEE Transactions on Medical Imaging*, Vol. 22, No. 2, 137-154, February 2003.
8. J. Damon, "Determining the Geometry of Boundaries of Objects from Medial Data," To appear, *International Journal of Computer Vision*, 2005.
9. D. Merck, S. Joshi, G. Tracton, and S.M. Pizer, "On Single Figure Statistical M-Rep Model Construction," *in preparation.*
10. Q. Han, C. Lu, G. Liu, S.M. Pizer, S. Joshi, and A. Thall, "Representing Multi-Figure Anatomical Objects," in *International Symposium on Biomedical Imaging*, pp. 1251-1254, Apr. 2004.
11. Q. Han, S.M. Pizer, D. Merck, S. Joshi, and JY. Jeong, "Multi-figure Anatomical Objects for Shape Statistics," To appear, *Information Processing in Medical Imaging (IPMI)*, 2005.
12. S.M. Pizer, P.T. Fletcher, S. Joshi, A.G. Gash, J. Stough, A. Thall, G. Tracton, and E.L. Chaney, "A Method and Software for Segmentation of Anatomic Object Ensembles by Deformable M-Reps," To appear, *Medical Physics*, 2005.
13. E. Chaney, S.M. Pizer, S. Joshi, R. Broadhurst, P.T. Fletcher, G. Gash, Q. Han, JY. Jeong, C. Lu, D. Merck, J. Stough, G. Tracton, MD J. Bechtel, J. Rosenman, YY. Chi, and K. Muller. "Automatic Male Pelvis Segmentation from CT Images via Statistically Trained Multi-Object Deformable M-rep Models," *Presented at American Society for Therapeutic Radiology and Oncology*, 2004.
14. S. Joshi, "Large Deformation Diffeomorphisms and Gaussian Random Fields for Statistical Characterization of Brain SubManifolds," PhD Thesis, Dept. of Electrical Engineering, Sever Institute of Technology, Washington Univ., Aug. 1997.
15. R.E. Broadhurst, J. Stough, S.M. Pizer, and E.L. Chaney, "Histogram Statistics of Local Image Regions for Object Segmentation," in *this volume, International Workshop on Deep Structure, Singularities and Computer Vision (DSSCV)*, 2005.